

Comparison of methods of determining meteoroid range rates from linear frequency modulated chirped pulses

R. Loveland,¹ A. Macdonell,¹ S. Close,² M. Oppenheim,³ and P. Colestock¹

Received 21 July 2010; revised 30 November 2010; accepted 11 January 2011; published 18 March 2011.

[1] In this paper we present three methods for evaluating range rates of meteoroids passing through the ionosphere, using linear frequency modulated (LFM) chirped pulse data from the ALTAIR radar. The first method is based on the simple calculation of range differences divided by interpulse intervals. The second method utilizes the dual-frequency capability of ALTAIR to solve for range rates based on the difference in the measured ranges due to range-Doppler coupling. The third method utilizes a simplified form of integer programming in order to unwrap the phase differences of the matched filter time response, with reliance on the rough approximation available from the first method to disambiguate the solution set. The results of the three methods, with error bounds, are given for a large set of meteoroid head echoes taken from a data collection conducted with ALTAIR in 2007.

Citation: Loveland, R., A. Macdonell, S. Close, M. Oppenheim, and P. Colestock (2011), Comparison of methods of determining meteoroid range rates from linear frequency modulated chirped pulses, *Radio Sci.*, 46, RS2007, doi:10.1029/2010RS004479.

1. Introduction

[2] Data taken with the ALTAIR radar can be used to determine a variety of types of information about meteoroids as they pass through the ionosphere [*Close et al.*, 2002; *Hunt et al.*, 2004]. The range rates (i.e., radial velocities from the radar) of the meteoroids are of particular interest, both in themselves and as a basis for determining densities, etc. in other calculations. In this paper we present a brief discussion of related techniques, followed by a description of the ALTAIR radar and data collection, and the details of three methods for calculating range rates: (1) simple differencing and division, (2) dual-frequency matching utilizing range-Doppler coupling, and (3) phase unwrapping of the matched filter time response. This is followed by a comparison of the

results of applying these methods to a large set of meteoroid head echoes.

2. Data

2.1. ALTAIR Radar

[3] ALTAIR is a 46 m diameter, high-power, two-frequency radar operating at 158 MHz (VHF) and 422 MHz (UHF). It resides in the central Pacific at 9°N and 167°E (geographic) on the island of Roi-Namur in the Kwajalein Atoll, Republic of the Marshall Islands. ALTAIR transmits a peak power of 6 MW simultaneously at the two frequencies with right-circularly (RC) polarized signal energy in a half power beam width of 2.8° and 1.1° at VHF and UHF, respectively. ALTAIR receives both right-circular and left-circular energy and has four additional receiving horns for the purpose of angle measurement, which gives the position of an object in three dimensions [*Close et al.*, 2000].

2.2. Data Collection Parameters

[4] The two ALTAIR waveforms used to collect the data were a VHF LFM chirped pulse with a 100 μ s pulse width (15 m range spacing), and a UHF LFM chirped pulse with a 400 μ s pulse width (also 15 m range spacing). A 8.7 ms pulse repetition interval (PRI) was utilized in this collection. Using these waveforms, ALTAIR can detect a target as small as -74 decibels relative to a

¹Los Alamos National Laboratory, Los Alamos, New Mexico, USA.

²Department of Aeronautics and Astronautics, Stanford University, Stanford, California, USA.

³Department of Astronomy, Boston University, Boston, Massachusetts, USA.

Table 1. Summary of Some of the UHF and VHF Data Collection Parameters^a

Parameter	VHF	UHF
T (μ s)	100	400
f_0 (MHz)	158	422
B (MHz)	7.06	5.00
PRI (ms)	8.6955	8.6955

^a T is the period of the LFM pulse, f_0 is the central frequency, B is the bandwidth, and PRI is the pulse repetition interval.

square meter (dBsm) at VHF and -80 dBsm at UHF at a range of 100 km. Few radars worldwide compare to the sensitivity achievable by ALTAIR [*Janches et al.*, 2008]. Table 1 summarizes some of the UHF and VHF data collect parameters.

3. Range Rate Calculation Methods

[5] Three different methods were used to calculate the range rates, varying widely in both complexity and generality.

3.1. Range Differencing Approach

[6] Range differencing is both the simplest and most general approach, with correspondingly lowest performance. In this case the range rate at time k , v_k , is estimated using (note that the effect of range-Doppler coupling is ignored because its effects are small here)

$$\hat{v}_k = \frac{r_k - r_{k-1}}{t_k - t_{k-1}} \equiv \Delta r_k / \Delta t_k, \quad (1)$$

where the r_k are the measured range values interpolated from the peak of the match filter response at time t_k , with Δt_k being the pulse repetition interval (PRI). Assuming uncorrelated errors between the range and PRI, the error is then approximated by [*Bevington*, 1969]

$$\sigma_{v_k} = \hat{v}_k \sqrt{\frac{\sigma_{\Delta r_k}^2}{\Delta r_k^2} + \frac{\sigma_{\Delta t}^2}{\Delta t^2}}. \quad (2)$$

For typical meteors $\sigma_{\Delta r_k} / \Delta r_k \approx 0.05$, while $\sigma_{\Delta t} / \Delta t \approx 1.15 \times 10^{-4}$, making the second term in equation (2) negligible. (The first approximation is based on the assumption that $\sigma_{\Delta r_k} \approx 1$ range bin, with Δr_k in the neighborhood of 20 range bins. The second approximation is probably quite conservative; the number given for the PRI has a value of 8.6955 ms, suggesting validity out

to at least the fourth decimal place, so we take $\sigma_{\Delta t} \approx 0.0001$ ms.) The error is then

$$\sigma_{v_k} = \hat{v}_k \left| \frac{\sigma_{\Delta r_k}}{\Delta r_k} \right| \approx 0.05 \hat{v}_k. \quad (3)$$

The results of this technique on an example meteoroid streak are shown in Figure 1. It should be noted that while the percentage error is relatively low, the extreme quantization makes the determination of higher derivatives difficult.

3.2. Dual-Frequency Approach

[7] It was previously mentioned that ALTAIR pulses simultaneously in both UHF and VHF. Returns are generally much stronger for VHF, but some meteors also have a strong return for UHF pulses. For these pulses with significant returns in both bands, it is possible to infer range rates from the differing shifts in range values caused by range-Doppler coupling (RDC) [*Cook and Bernfeld*, 1967].

[8] RDC is an artifact of the LFM pulse compression scheme, which results in a shift in the measured range value of [*Mahafza*, 1998]

$$\delta_r = \frac{T_x f_{0,x} v_x}{B_x} \equiv c_x v, \quad (4)$$

where the subscript x represents either UHF or VHF values. These are combined into the constant c_x for notational convenience. The measured range values are then

$$r_{x,k} = \check{r}_k - c_x v_k, \quad (5)$$

where the \check{r}_k are the true range values. Knowing that while the $r_{x,k}$ and $c_{x,k}$ vary between UHF and VHF, the ranges \check{r}_k and range rates v_k are identical, we use equation (5) to estimate

$$\hat{v}_k = \frac{r_{\text{VHF},k} - r_{\text{UHF},k}}{c_{\text{VHF}} - c_{\text{UHF}}} \equiv \frac{\Delta r_{d,k}}{c_{\text{VHF}} - c_{\text{UHF}}} \approx 31.72 \text{ s}^{-1} \cdot \Delta r_{d,k}. \quad (6)$$

Note that while the previous range differencing technique used a Δr_k based on measurements from times k and $k-1$, the $\Delta r_{d,k}$ here is based on UHF and VHF measurements taken simultaneously at time k .

[9] Using a process similar to that conducted previously to find the error, assuming that the values underlying the constants c_x are precisely known compared to the range uncertainties, we obtain

$$\sigma_{v_{d,k}} = \hat{v}_k \left| \frac{\sigma_{\Delta r_{d,k}}}{\Delta r_{d,k}} \right|. \quad (7)$$

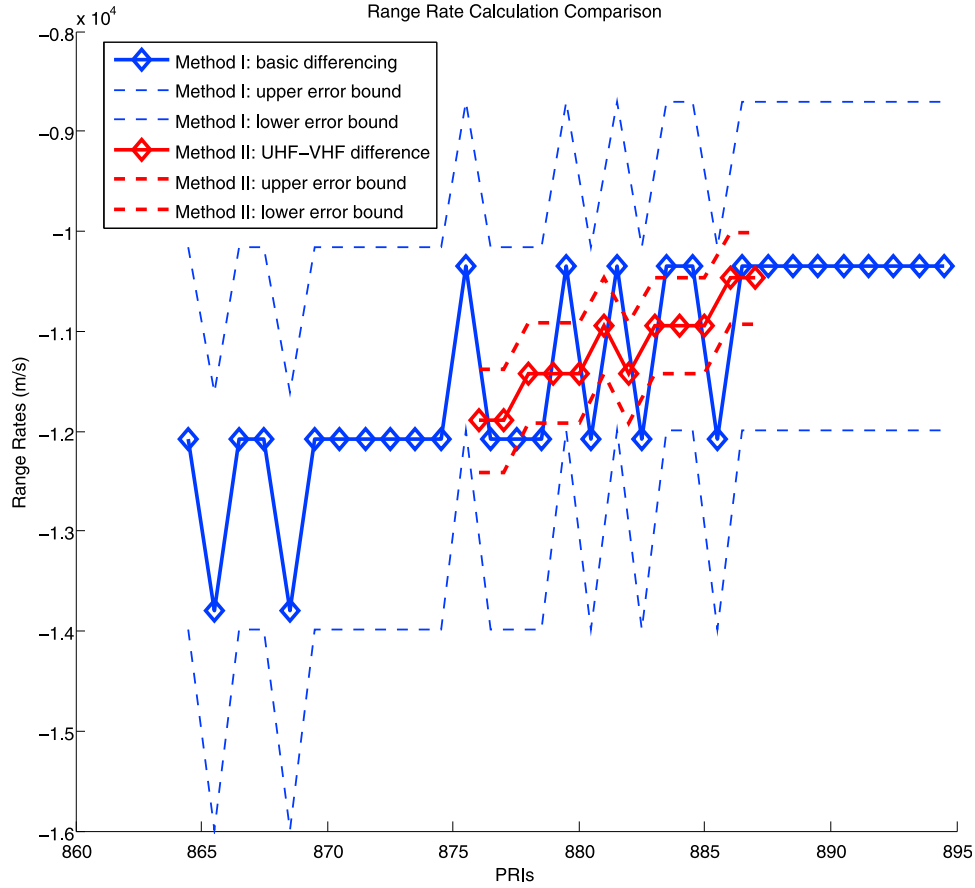


Figure 1. Range rates arrived at using the previously described methods, with 1σ error bars. Blue lines are based on simple range differencing, while red lines are the result of the dual-frequency approach.

We can relate this error estimate to that of the previous technique by relating the error σ and range Δ .

[10] Since the same noise affects the correct estimate of the return pulse peak locations in both cases, $\sigma_{\Delta r_{d,k}} = \sigma_{\Delta r_k}$. Fortunately, however, $\Delta r_{d,k}$ is larger than Δr_k by about a factor of 4. To see this, consider that for a given range rate, with no noise,

$$v_k = \frac{\Delta r_k}{\Delta t_k} = \frac{\Delta r_{d,k}}{c_{\text{VHF}} - c_{\text{UHF}}}. \quad (8)$$

Rearranging,

$$\Delta r_{d,k} = \frac{c_{\text{VHF}} - c_{\text{UHF}}}{\Delta t_k} \cdot \Delta r_k \approx 3.627 \cdot \Delta r_k. \quad (9)$$

The relation between σ_{v_d} and σ_{v_k} is then found using equations (3) and (7) to be

$$\sigma_{v_d} = \frac{\Delta t_k}{c_{\text{VHF}} - c_{\text{UHF}}} \sigma_{v_k} \approx 0.276 \cdot \sigma_{v_k}, \quad (10)$$

resulting in an error reduction of about a factor of 4 from the simple differencing technique. This is clearly an improvement, but it should be noted that the applicability of this technique is limited to those cases where the signal-to-noise ratio (SNR) is high enough in both UHF and VHF to allow the detection of the meteoroid. In practice this limitation is severe enough to make this approach of limited value.

[11] The results of this technique on an example meteoroid streak are shown in Figure 1. It is clear that this is an improvement on the results of the first method, but that the quantization is still a problem for determining higher-order derivatives.

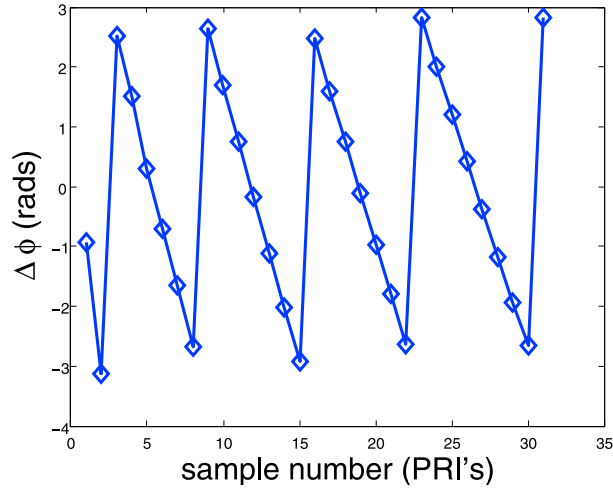


Figure 2. $\Delta\phi$ values for a meteoroid with particularly slow (and constant) decelerations between pulses. Note the easily discernible wrapping points.

3.3. Phase Unwrapping Approach

3.3.1. Background

3.3.1.1. Intrapulse Doppler

[12] The two approaches discussed previously are based on using range values inferred from the location of the peak of the magnitudes of the matched filter time response, $y(t)$, given by *Skolnik* [2008] as

$$y(t) = [1 - |t/T|] \text{sinc}[(f_d + \alpha t)T(1 - |t/T|)] \cdot \dots \cdot \text{rect}(t/2T)e^{j\pi f_d t}. \quad (11)$$

Note that the location of the peak utilizes only the magnitude of equation (11). The phase,

$$\phi = \pi \cdot f_d \cdot t, \quad (12)$$

also contains information about the velocity through f_d , the Doppler frequency shift, which is related to the range rate by $f_d = 2 \cdot v/\lambda$, where λ is the central wavelength of the LFM pulse.

[13] Unfortunately, intrapulse phase variation that can be meaningfully determined from samples with sufficiently high SNR is too low to be useful. To see this consider the following scenario with typical values. For a typical meteoroid with range rate of ~ 40 km/s, with a VHF center frequency of 158 MHz, we obtain a Doppler frequency of ~ 42 kHz, with a corresponding Doppler period of ~ 23 μ s. We find that in practice in the data the portion of the matched filter return that can be discerned above the noise floor is ~ 250 ns long; this corresponds to the length of time during which a meaningful phase value

can be measured. Then, given that the ratio of this length of time to the Doppler period is about 0.01 for the given scenario, we expect to see a roughly constant phase from the matched filter return for a given pulse. This matches what is seen in the data.

3.3.1.2. Interpulse Doppler

[14] Between pulses, however, the phase change is quite significant for the same scenario. From *Skolnik* [2008], the phase change due to the Doppler shift is

$$\frac{d\phi}{dt} = \frac{4\pi v}{\lambda}. \quad (13)$$

Rearranging, inserting frequency, and using the sampling interval T (i.e., the PRI), the formula relating $\Delta\phi$, the phase difference between two adjacent pulses, to the range rate, v , is given by

$$\Delta\phi = \text{mod}\left(\frac{4\pi f_0 T v}{c}, 2\pi\right), \quad (14)$$

where c is the speed of light. The $\text{mod}()$ operation is included because we are dealing with phase; it must be reversed by “unwrapping” in order to find v .

[15] Using the example scenario values, we expect a phase change of ~ 2300 rad between pulses. This level of wrap is unsurprising and is in good agreement with the well known ambiguities arising in range and/or Doppler as a result of various choices of PRI. Methods for addressing these ambiguities using multiple PRI waveforms are discussed by, for example, *Trunk and Brockett* [1993] and *Trunk and Kim* [1994]. These data were acquired well in advance of our analysis, however, so that no waveform modification could be performed.

[16] The interpulse phase change is clearly large enough to be problematic to unwrap, but knowing that the change in velocity is small, we can expect nearly all of this to remain constant over the streak. Due to the $\text{mod}()$, this constant will only show as a remainder with value $< 2\pi$. If we concentrate instead on Δv ,

$$\Delta^2\phi = \Delta\phi_i - \Delta\phi_{i-1} \quad (15)$$

$$\Delta^2\phi = \text{mod}\left(\frac{4\pi f_0 T \Delta v}{c}, 2\pi\right). \quad (16)$$

Based on a meteoroid with approximately 4 km/s Δv over 35 samples, a representative Δv over a single PRI is ≈ 117 m/s. Using equation (16), neglecting the $\text{mod}()$, we obtain $\Delta^2\phi \approx 6.7$ rad. Thus we see that the actual change in $\Delta\phi$ values between samples is low enough to allow for the possibility of unwrapping. The $\Delta\phi$ of a particularly slowly decelerating meteoroid is used to illustrate this in Figure 2.

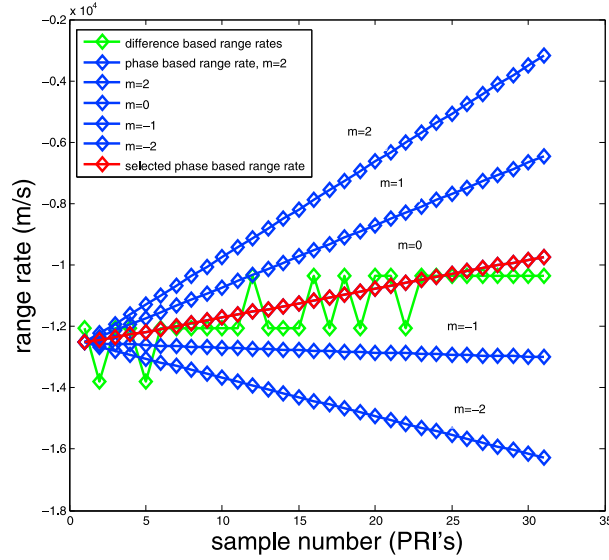


Figure 3. Range rates arrived at using the previously described method. The green line is the heavily quantized difference-based solution, while the blue lines are the possibilities resulting from different values of m , with the red line showing the final solution.

3.3.2. Algorithm

[17] Section 3.3.1 illustrates that it may be possible to find a solution for the overall range rate curve by determining individual Δv , and subsequently combining these together. In order to do this, the associated $\Delta^2 \phi$ must be unwrapped. To accomplish this, we can utilize two constraints resulting from the underlying physics: (1) the range rate curve must be smooth, and (2) the curve should roughly match the results of the range differencing approach. This in turn suggests a two-step approach of (1) unwrapping the phase to arrive at a family of possible answers which satisfy the smoothness criterion and (2) using the results of the range differencing approach to select the single correct answer.

[18] The desired answer is a set of k_i , $k_i \in \mathcal{K}$, $i \in \{1..N\}$, with N equal to the number of samples in the streak, such that

$$\Delta \check{\phi}_i = \Delta \phi_i + k_i \cdot 2\pi. \quad (17)$$

[19] The smoothness constraint is addressed first by minimizing the higher-order derivatives. Specifically, we

[20] 1. Let $k_1, k_2 = 0$.

[21] 2. For $i = 3..N$, step 1 find the slopes $\Delta^2 \phi_{i-1}$ and $\Delta^2 \phi_i$, step 2, over a range of $j \in \{-10..10\}$, find j^* such that $\|(\Delta^2 \phi_i + j2\pi) - \Delta^2 \phi_{i-1}\|$ is minimized and step 3, let $\{k_i..k_N\} = \{k_i..k_N\} + j^*$.

[22] Note that step 3, which adds the correction to both the current and all successive points, is effectively equivalent to an integration. This results in a smooth curve of $\Delta \check{\phi}_i$, but there are other curves that are equally smooth that can be arrived at by adding in lines with slopes of integer multiples of 2π . Thus, an entire family of solutions exist,

$$\Delta \check{\phi}_i^{(m)} = \Delta \check{\phi}_i + m \cdot (i - 1) \cdot 2\pi. \quad (18)$$

Since wrapping is limited to multiples of 2π , m must be an integer, and the guaranteed low values of deceleration constrain it to be small.

[23] The proper value for m can be found by finding the corresponding solution for v that best matches the rough range rates arrived at using the differencing method. In order to do this, a v_0 must be estimated, since the previous technique is based on integrating Δv and therefore does not provide this. For now this is estimated by simply averaging the first four points of the rough range rates, designated v_R , so

$$v_0 = \frac{\sum_{i=1}^4 v_{R,i}}{4}. \quad (19)$$

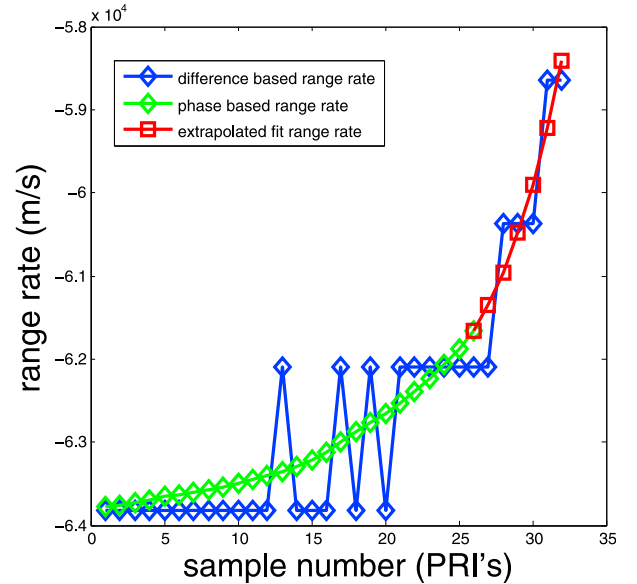


Figure 4. The phase-based range rates for a streak are shown in green, followed by the fitted range rates shown in red.

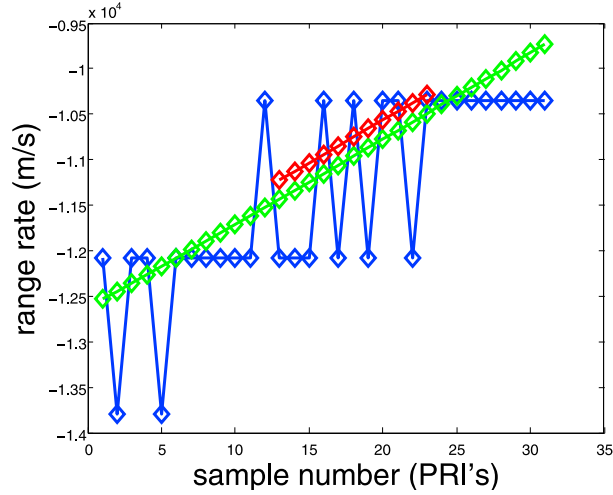


Figure 5. Independent comparison of the results of the phase-based method for UHF (in red) and VHF (in green). Note the good agreement, excluding the v_0 offset.

The solution for m is then found by minimizing the RMS error between phase-based and rough differencing range rates, over m ,

$$m^* = \operatorname{argmax}_{m \in \{-4.4\}} \sqrt{\sum_{i=1}^N \left(\frac{c\Delta\check{\phi}_i^{(m)}}{4\pi f_0 T} - v_{R,i} \right)^2}. \quad (20)$$

Finally, this results in a range rate curve solution of

$$v_i = \frac{c\Delta\check{\phi}_i^{(m^*)}}{4\pi f_0 T} + v_0. \quad (21)$$

The results of this process are shown in Figure 3. The red line is the final selected range rate solution.

[24] It was experimentally observed that for a few meteoroids with particularly large changes in deceleration the smoothness assumption breaks down. In order to counter the resulting ambiguity in k_i selection, a check was inserted into the algorithm which stops the phase unwrapping method when the difference between the two closest answers for adjacent k_i values becomes < 0.5 rad/(PRI) 2 . The final answer is then constructed by fitting a fifth-order polynomial to the combined set of valid unwrapped points and difference based $v_{R,i}$ for the remainder of the streak. An example streak illustrating this is shown in Figure 4.

3.3.3. Validation Case

[25] As a check on the validity of the algorithm we tried using it independently in both UHF and VHF on a special case with sufficient signal strength in UHF. The results are shown in Figure 5; agreement is good with both bands producing nearly identical results for deceleration. The slight vertical offset between the two results from a combination of slightly different v_0 values and RDC.

[26] It should be noted that the phase-based method is more liable to fail in the first part of the algorithm (i.e., the initial unwrapping) in UHF. This is because the constant for UHF used in equation (14) is larger than that for VHF by a factor of 2.7, which in turn makes $\Delta\phi$ greater for a given value of Δv and thus easier to confuse with a corresponding wrapped possibility.

3.3.4. Error Analysis

[27] Two kinds of errors occur with the phase-based technique. The first is catastrophic, in the sense that if the wrong value of k_i is selected early in the streak, or an ambiguity occurs which results in an early termination of the phase-based method, the resulting range rate estimate is totally wrong. These types of errors are mostly discernible by eye; a particularly obvious example is shown in Figure 6.

[28] The second type of error is much smaller, occurring as a result of misestimating v_0 , combined with noise in the phase measurements. If we assume that v_0 induced error is much larger than the phase measurement induced error, and that v_0 was basically constant over the first 4 mea-

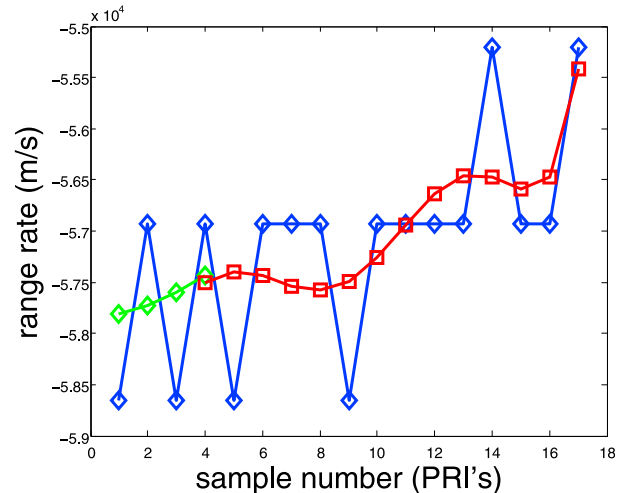


Figure 6. A wholly incorrect answer from the phase-based method is shown in green and red, with initial ambiguity resulting in an early termination, an incorrect selection for m^* and a following incorrect fit.

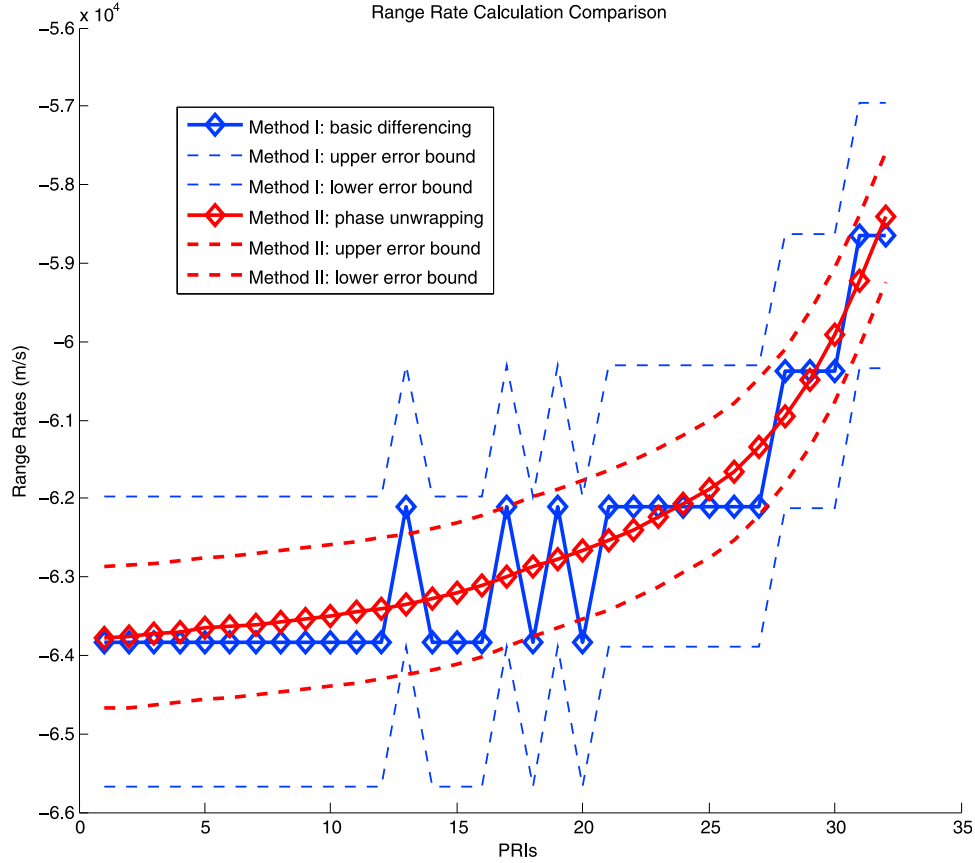


Figure 7. Range rates arrived at using the previously described methods, with 1σ error bars. The blue lines are based on simple range differencing, while the red lines are the result of the phase unwrapping approach.

surements, then the error corresponding to equation (19) becomes

$$\sigma_{v_0} \approx \frac{\hat{v}_0}{4} \sqrt{\frac{\sigma_{\Delta r_0}^2}{\Delta r_0^2} + \frac{\sigma_{\Delta r_3}^2}{\Delta r_3^2}} \quad (22)$$

$$\sigma_{v_0} \approx \frac{\hat{v}_0}{2} \left| \frac{\sigma_{\Delta r_k}}{\Delta r_k} \right|. \quad (23)$$

Figure 7 shows the 1σ error bars for the differencing method and the phase method for a given meteoroid trace based on these assumptions.

[29] Also of interest is the deceleration (i.e., Δv) error, which has no v_0 component overshadowing the noise of the phase measurement. Making a good estimate of this is difficult because (1) there is no “ground truth” available through alternative data from direct measurements, (2) there is no sufficiently specific analytical form

available to fit the range curve to, and (3) $\sigma_{\Delta\phi}$ is a (an unknown) function of the SNR. A characterization of the relation between $\sigma_{\Delta\phi}$ and the SNR might be addressed using the observed intrapulse phase variation, however, a full investigation of this cannot be supported as part of the current effort, and will therefore be postponed.

4. Conclusion

[30] The evaluation of meteoroid range rates is necessary in order to calculate a variety of meteoroid characteristics including mass, density, etc. In this work we have presented three methods and have shown that the novel interpulse Doppler approach in particular provides unprecedented measurement of velocities and accelerations.

[31] Future work will include an investigation of the interpulse Doppler method’s error dependence on SNR so that proper error bounds can be found for both velocity and acceleration. Application of the method to a

large number of meteoroids will also be conducted in order to examine statistical results for a large population. Algorithmic improvements will also be investigated in order to overcome the current breakdown of the method when accelerations become too large. Starting the $\Delta\phi$ calculation from the middle of the streak will also be investigated in order to mitigate the sensitivity of the technique to the low SNR values present at the ends of the streak.

[32] **Acknowledgments.** The authors would like to acknowledge the provision of data by William Cooke of the NASA Marshall Space Flight Center and the Los Alamos National Laboratory LDRD office for funding this effort.

References

- Bevington, P. R. (1969), *Data Reduction and Error Analysis for the Physical Sciences*, McGraw-Hill, New York.
- Close, S., S. M. Hunt, M. Minardi, and F. M. McKeen (2000), Meteor shower characterization at Kwajalein Missile Range, *Lincoln Lab. J.*, 12, 33–43.
- Close, S., S. M. Hunt, F. M. McKeen, and M. J. Minardi (2002), Characterization of Leonid meteor head echo data collected using the VHF-UHF Advanced Research Projects Agency Long-Range Tracking and Instrumentation Radar (ALTAIR), *Radio Sci.*, 37(1), 1009, doi:10.1029/2000RS002602.
- Cook, C. E., and M. Bernfeld (1967), *Radar Signals: An Introduction to Theory and Application*, Academic, New York.
- Hunt, S. M., M. Oppenheim, S. Close, P. G. Brown, F. McKeen, and M. Minardi (2004), Determination of the meteoroid velocity distribution at the Earth using high gain radar, *Icarus*, 168, 34–42, doi:10.1016/j.icarus.2003.08.006.
- Janches, D., S. Close, and J. T. Fentzke (2008), A comparison of detection sensitivity between ALTAIR and Arecibo meteor observations: Can high power and large aperture radars detect low velocity meteor head-echoes, *Icarus*, 193, 105–111, doi:10.1016/j.icarus.2007.08.022.
- Mahafza, B. R. (1998), *Introduction to Radar Analysis*, CRC Press, Boca Raton, Fla.
- Skolnik, M. (2008), *Radar Handbook*, 3rd ed., McGraw-Hill, New York.
- Trunk, G. V., and S. Brockett (1993), Range and velocity ambiguity resolution, paper presented at IEEE National Radar Conference, Boston, Mass.
- Trunk, G. V., and M. W. Kim (1994), Ambiguity resolution of multiple targets using pulse-Doppler waveforms, *IEEE Trans. Aerosp. Electron. Syst.*, 30, 1130–1137, doi:10.1109/7.328789.
- S. Close, Department of Aeronautics and Astronautics, Stanford University, 496 Lomita Mall, Stanford, CA 94305-4035, USA.
- P. Colestock, R. Loveland, and A. Macdonell, ISR-2, Los Alamos National Laboratory, PO Box 1663, MS D436, Los Alamos, NM 87545, USA. (rohan@lanl.gov)
- M. Oppenheim, Department of Astronomy, Boston University, 725 Commonwealth Ave., Boston, MA 02215, USA.